Cell-Penetrating, Guanidinium-Rich Oligophosphoesters: Effective and Versatile Molecular Transporters for Drug and Probe Delivery

Colin J. McKinlay, Robert M. Waymouth,* and Paul A. Wender*

J. Am. Chem. Soc. **2016**, Article ASAP DOI: 10.1021/jacs.5b13452

Wipf Group Current Literature

Chaemin Lim

03/12/2016

Guanidinium-Rich Molecular Transporters

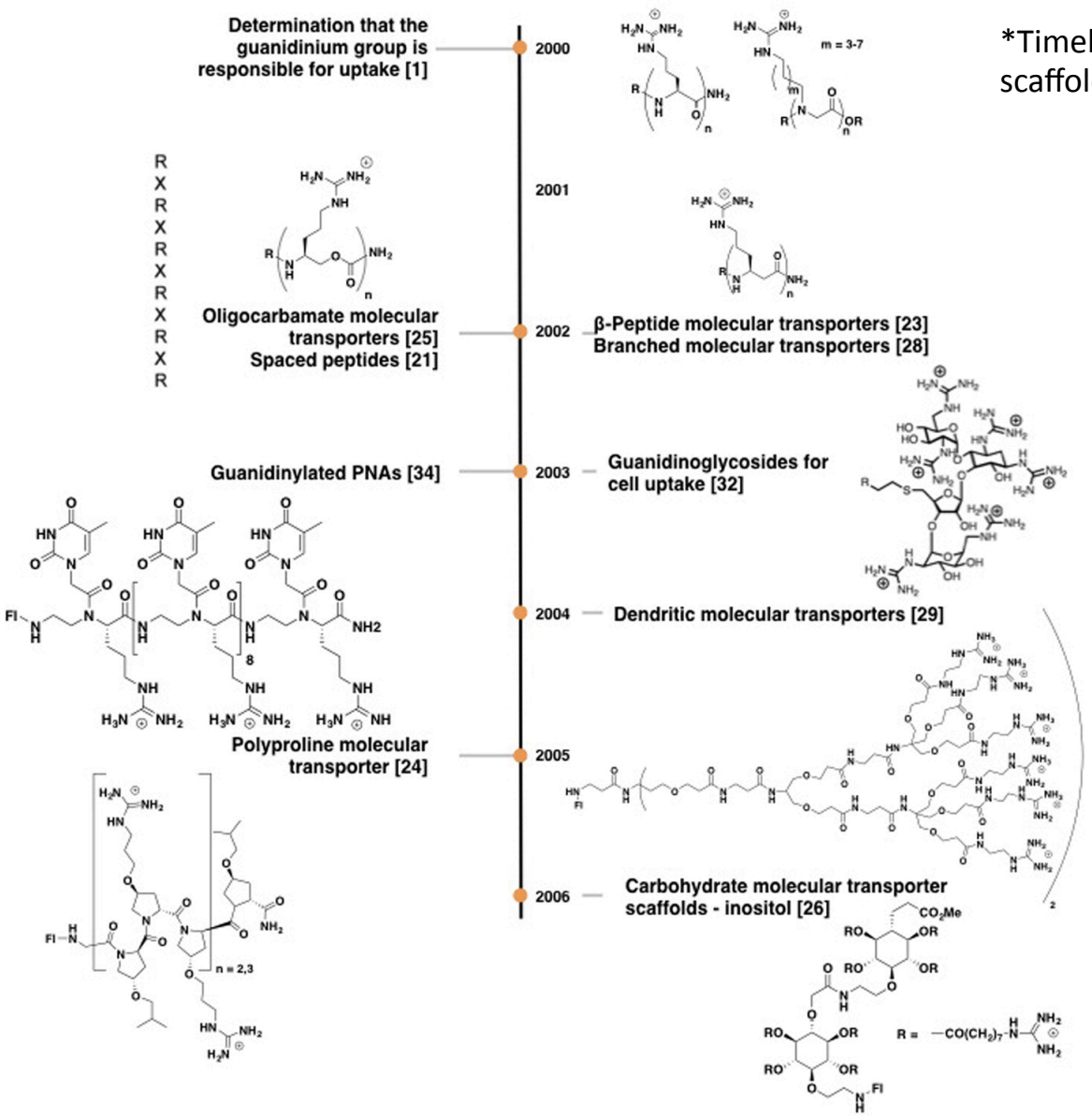

*Timeline for the development of different scaffolds for guanidinium-rich transporters

These transporters have been shown to enable or enhance the passage of numerous cargos including small molecules, peptides and proteins, and oligonucleotides.

Acc. Chem. Res., **2013**, *46*, 2944–2954.

Guanidinium-Rich Molecular Transporters

**Initially inspired by HIV-1 Tat protein*

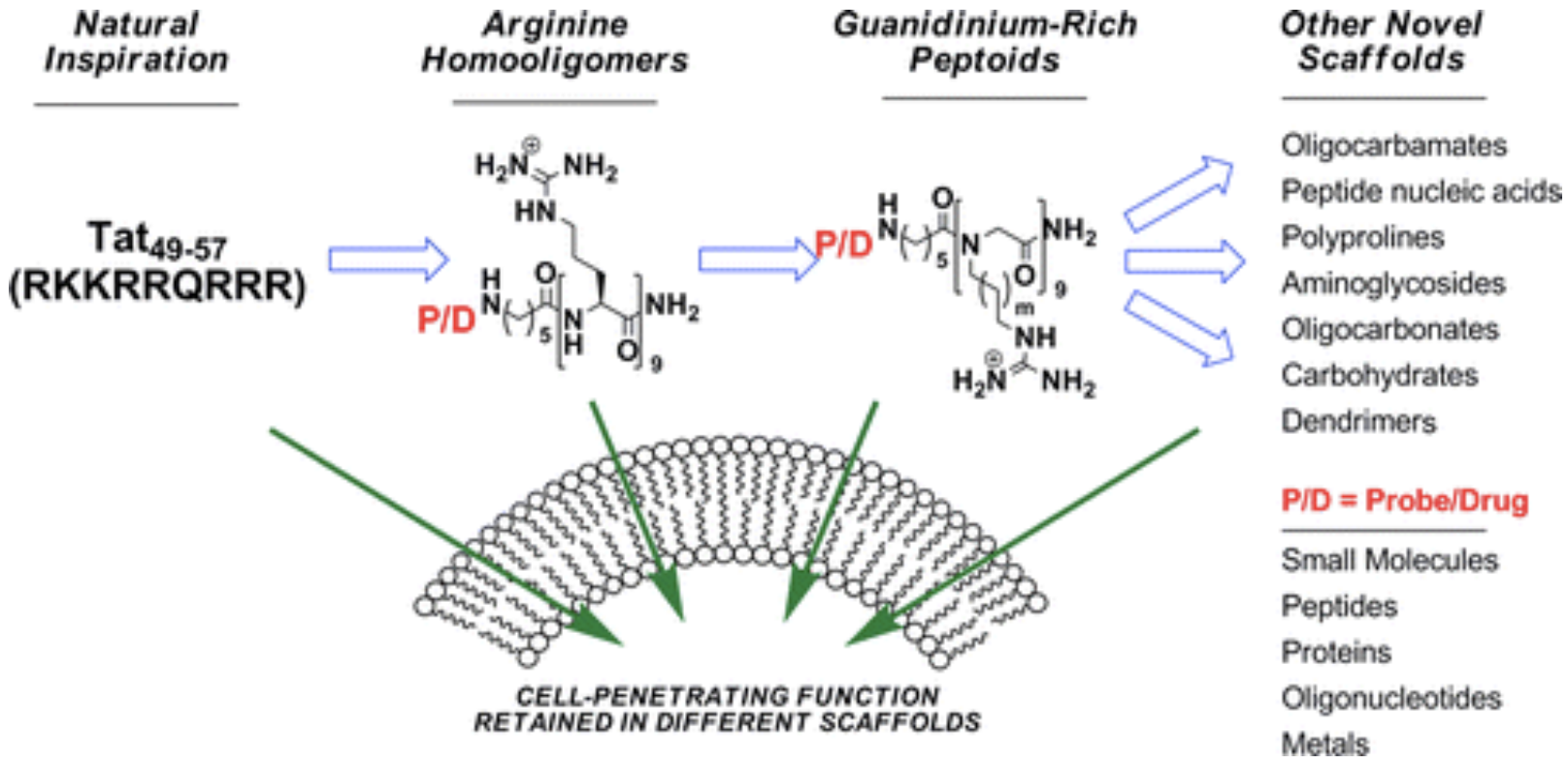

1988 – Discovery that HIV-Tat crosses the cell membrane.
1997 – Discovery that the HIV Tat 9-mer facilitates uptake.

Acc. Chem. Res., **2013**, *46*, 2944–2954.

Mechanism of uptake: adaptive translocation and endocytosis

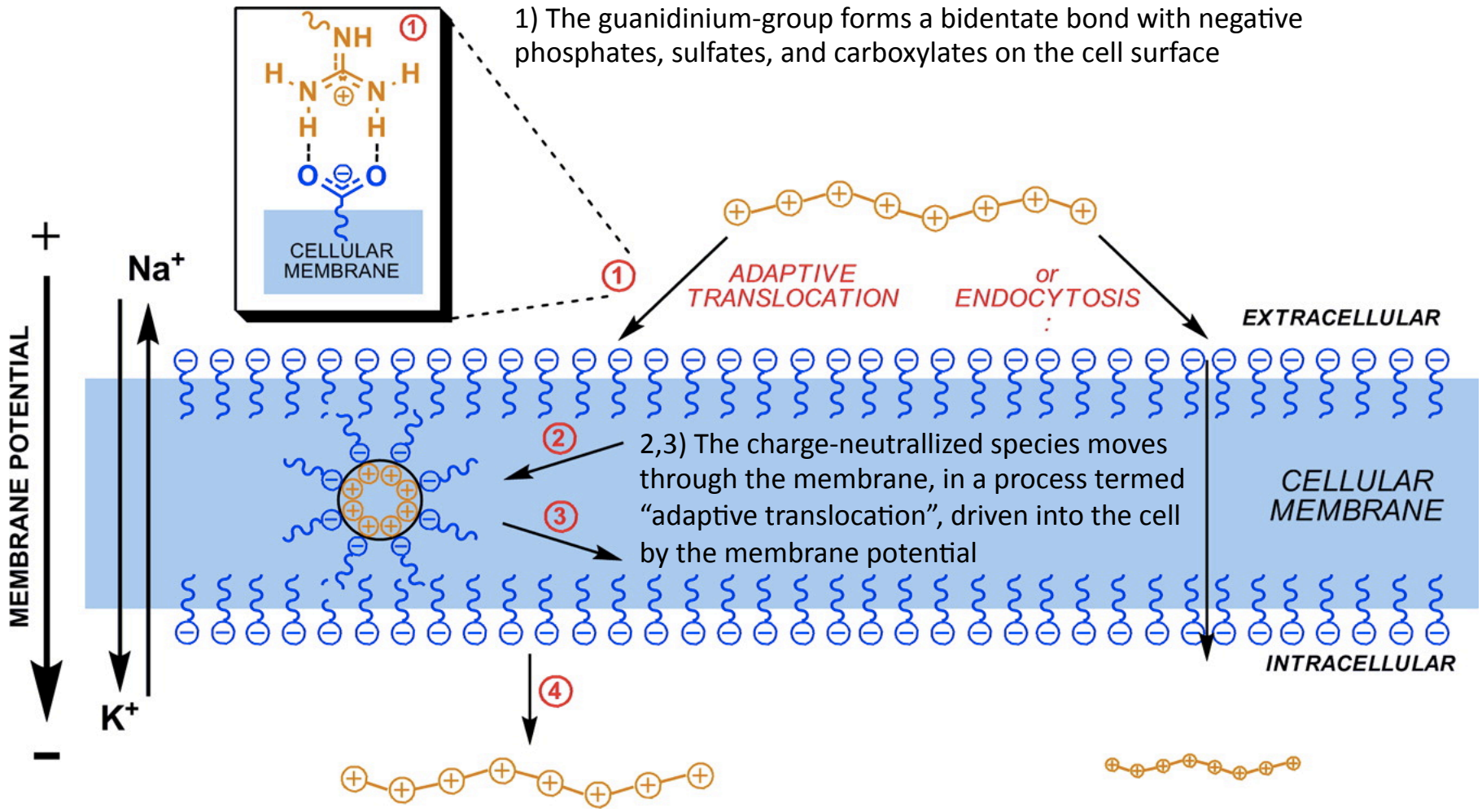

Diverse Guanidinium-Rich Scaffolds

- Peptoids, spaced peptides, oligocarbamates, dendrimers, and oligocarbonates are able to efficiently enter cells.

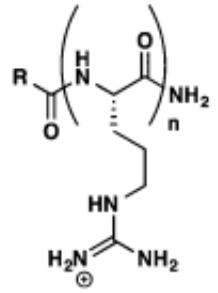

Oligoarginine peptide scaffold (2000)

increase step-economy

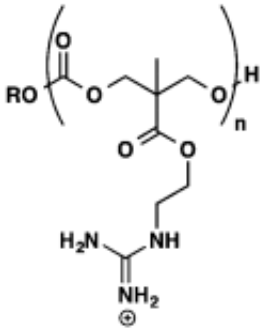

Methyl(trimethylene)carbonate (MTC) scaffod (2009)

increase functionality

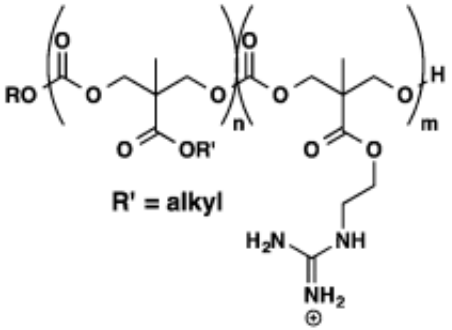

Amphipathic block MTC co-oligomers (2012)

increase stability

increase biocompatibility

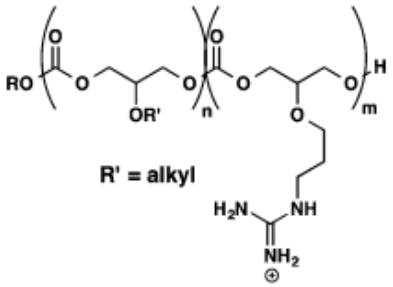

1,3-glycerol carbonate scaffold (2015)

Nat. Med. **2010**, *6*, 1253−1257.
J. Am. Chem. Soc. **2009**, *131*, 16401−16403.
Proc. Natl. Acad. Sci. U.S.A. **2012**, *109*, 13171−13176.
Mol. Pharmaceutics **2015**, *12*, 742−750.

In this study

A new class of molecular transporters, guanidinium-rich oligophosphoesters, which exhibit increased delivery efficacy and offer several advantages over previously reported systems.

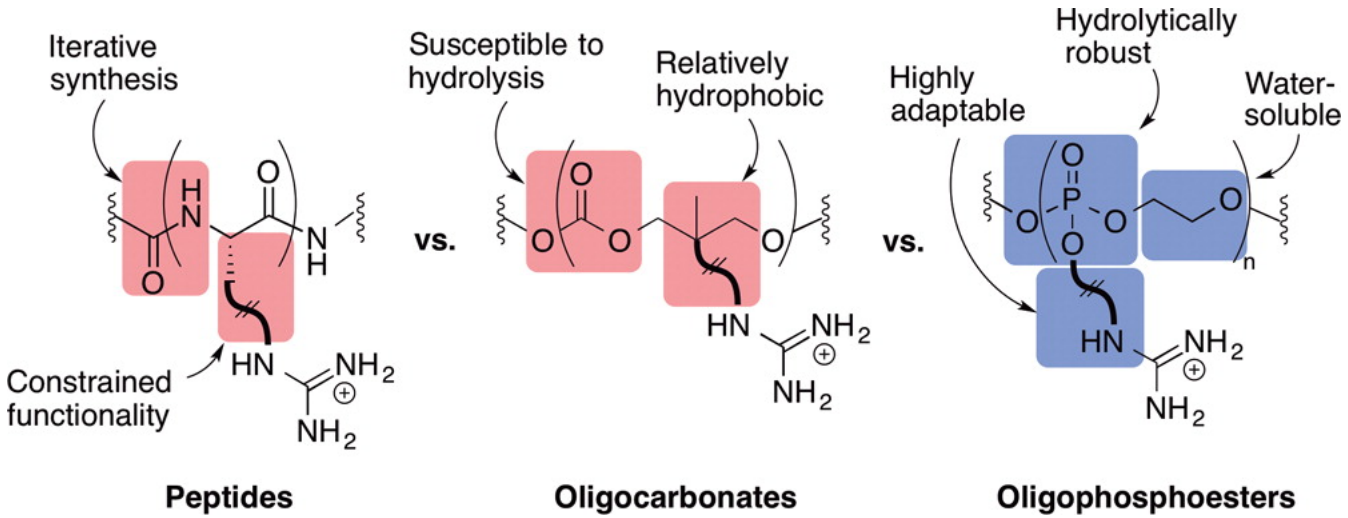

Comparison of select oligomeric scaffolds for drug delivery to the oligophosphoesters described in this work, specifically highlighting ease of synthesis, backbone hydrophilicity, structural diversity, and aqueous stability.

J. Am. Chem. Soc. Ahead of Print DOI: 10.1021/jacs.5b13452

Synthetic Polyphosphoesters (PPEs)

- Phosphorous containing polymers with repeated phosphoester linkages in the backbone
- PPE chemistry was pioneered by Penczek and co-workers in the 1970s

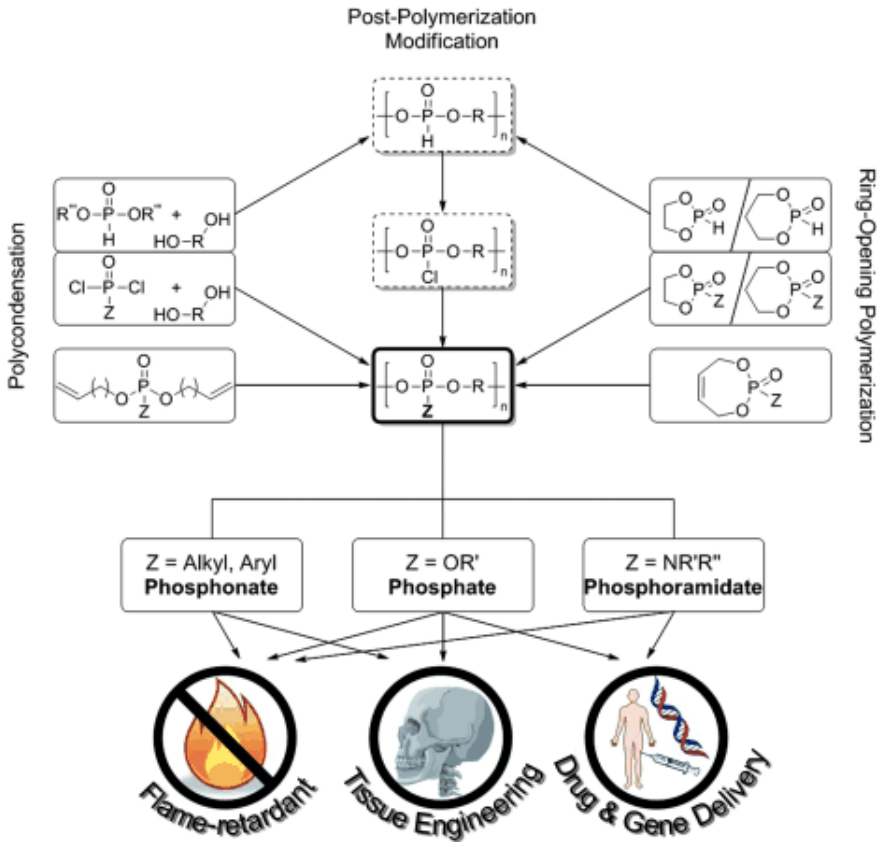

Synthetic pathways towards PPEs and major fields of application.

- High degradability
- Good biocompatibility
- Similarity to bio-macromolecules such as nucleic acids

Angew.Chem. Int. Ed. **2015**, *54*, 6098–6108.

Design and Synthesis: Monomer preparation & Oligomerization

- Guanidinium-Functionalized Cyclic Phospholane Monomer

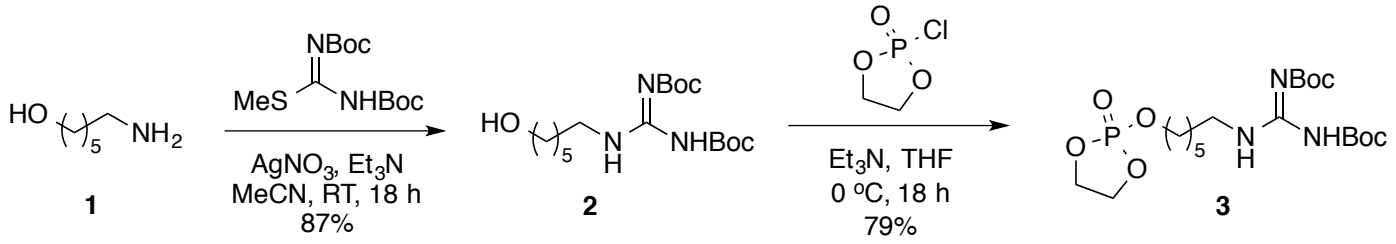

- Oligomerization of Hexyl-guanidinium Phospholane (HexPhos) Monomer

: Organocatalytic ring opening polymerization (OROP)

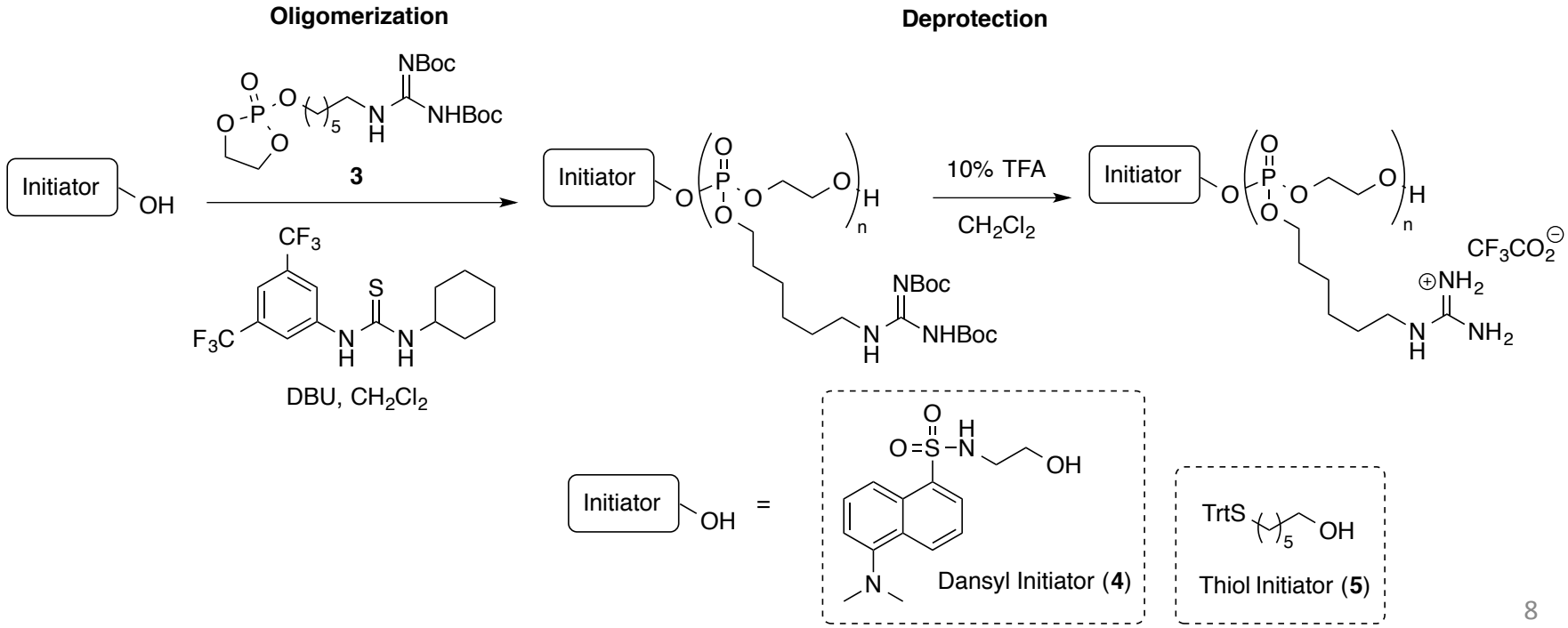

8

Design and Synthesis: Monomer preparation & Oligomerization

- Oligomerization of Hexyl-guanidinium Phospholane (HexPhos) Monomer
: Simple, one-flask procedure, oligomers of a variety of lengths were synthesized by controlling the initiator (**4** or **5**) to monomer (**3**) ratio.

Table 1. Guanidinium-Functionalized Oligomers Synthesized by Organocatalytic Ring-Opening Oligomerization

entry	initiator	DP (NMR)[a]	M_n (GPC)[b]	M_w/M_n (GPC)[b]
6a	Dansyl (4)	8	2537	1.31
6b	Dansyl (4)	10	2718	1.42
6c	Dansyl (4)	12	3262	1.22
6d	Dansyl (4)	18	3594	1.31
6e	Dansyl (4)	25	3472	1.38
7	Trityl-hexyl (5)	8	2838	1.37

[a]DP calculated by end group analysis. [b]M_n and M_w/M_n determined for protected oligomers by gel permeation chromatography (GPC) in THF relative to polystyrene standards

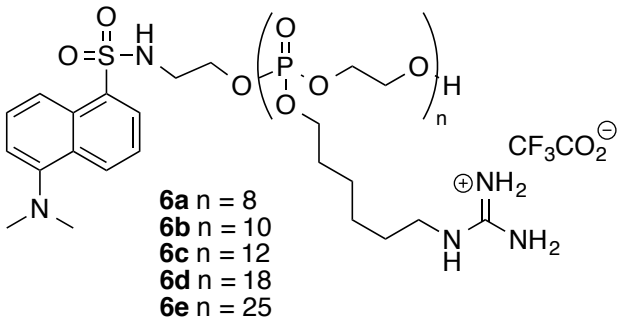

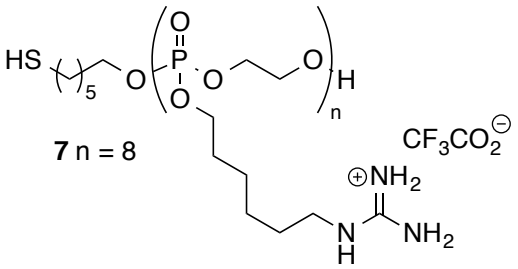

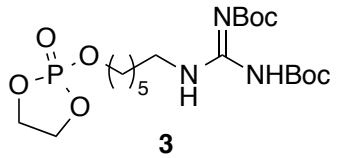

3

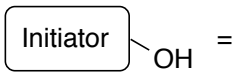

=

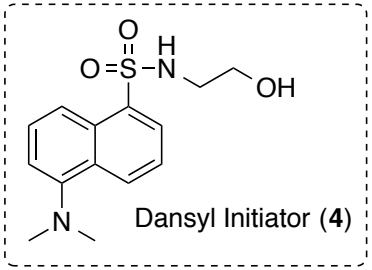

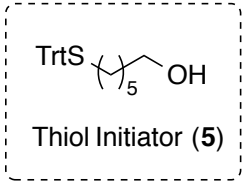

9

Hydrolytic Stability of HexPhos Oligomers

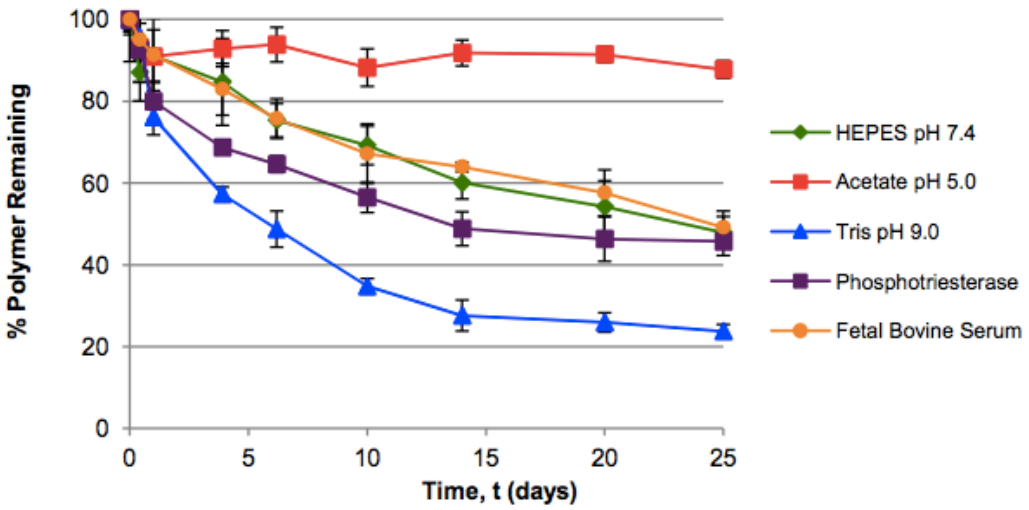

Increased hydrolytic and biological stability relative to oligocarbonates ($t_{1/2}$ = 8 h) and oligoesters ($t_{1/2}$ = 1-3 h)

Figure S5. Relative rates of hydrolysis of HexPhos oligomer **6d** as measured by ^{31}P NMR in different buffers. All incubations were done at 35 °C.

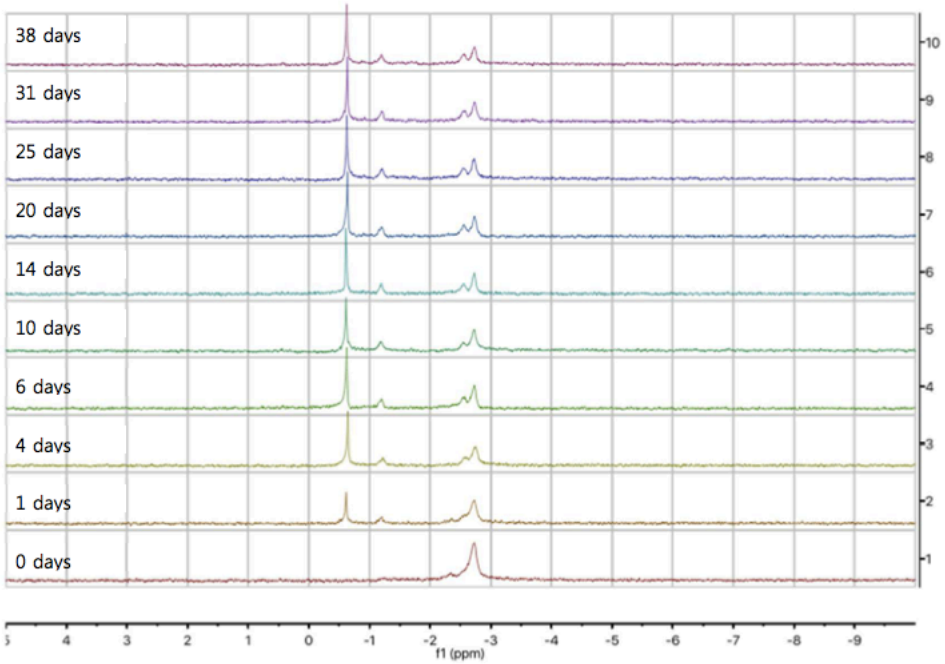

Figure S6. Representative ^{31}P NMR spectra of hydrolysis of HexPhos25 oligomer in Tris-EDTA buffer over time. The peak at δ = -2.7 represents the starting oligophosphoester, while new peaks at approx. -2.25, -0.9, and -0.5 represent hydrolysis products.

Cellular Uptake of HexPhos Molecular Transporters

A

Length Depepdence (in Hela cells)

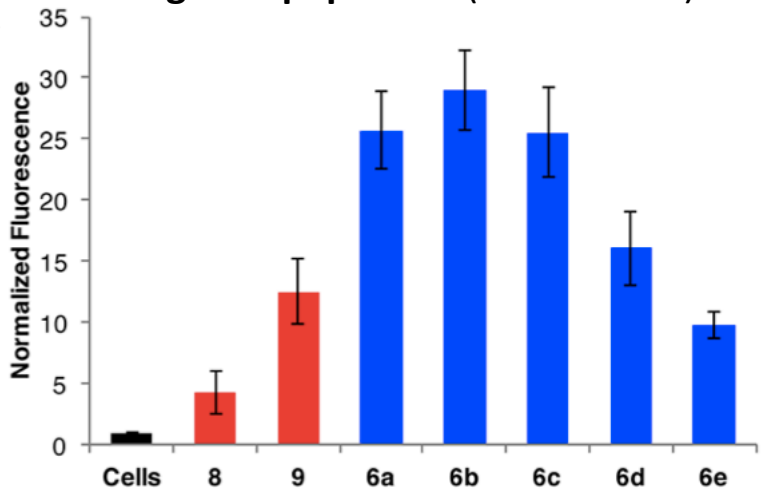

B

Cell Line Dependence

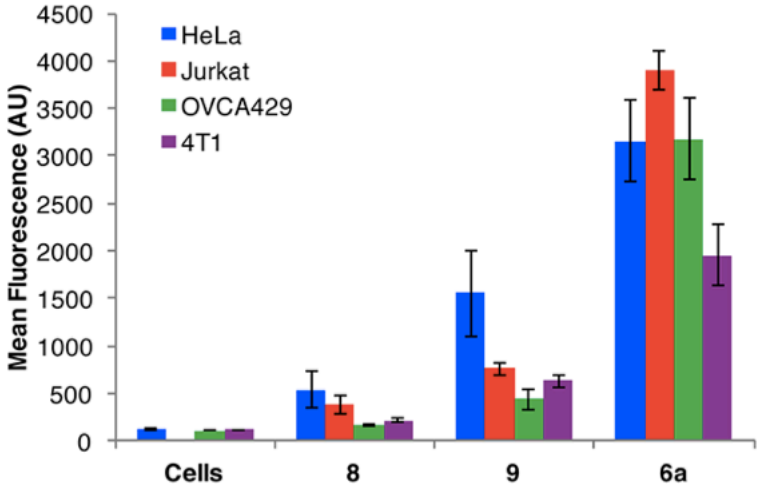

C

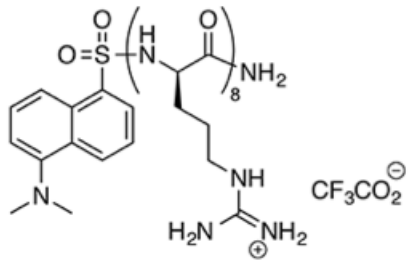

Dansyl-Arg$_8$ (**8**)

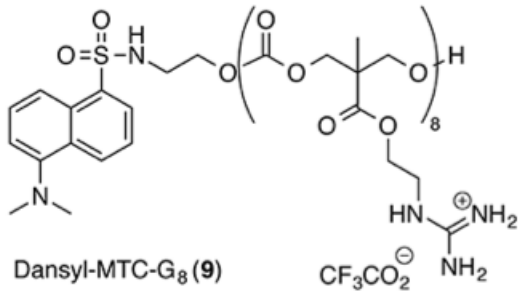

Dansyl-MTC-G$_8$ (**9**)

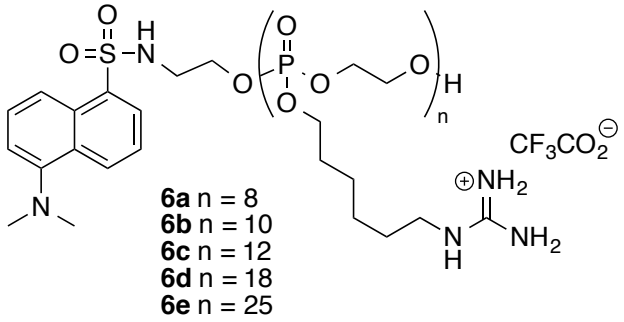

6a n = 8
6b n = 10
6c n = 12
6d n = 18
6e n = 25

11

Cellular Uptake and Toxicity of HexPhos Oligomers

Dose Depepdence

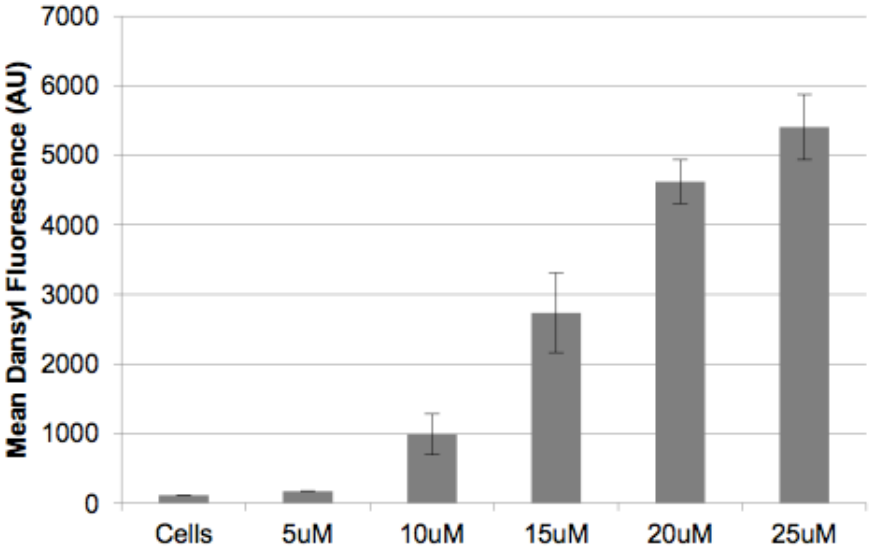

Figure S8. Concentration dependence of uptake of Dansyl-HexPhos8 oligomer **6a** in HeLa cells.

Cellular Toxicity

Compound	LD_{50} (μM) HeLa cells
Dansyl-MTC-G8 (**9**)	36.04 ± 5.55
Dansyl-HexPhos8 (**6a**)	18.03 ± 1.72
Dansyl-HexPhos10 (**6b**)	11.58 ± 1.60
Dansyl-HexPhos12 (**6c**)	9.54 ± 1.23
Dansyl-HexPhos18 (**6d**)	6.40 ± 2.28
Dansyl-HexPhos25 (**6e**)	3.44 ± 0.48

Figure S9. Compiled MTT-determined LD_{50} (the amount of compound required to reduce cellular viability by half) values for HexPhos oligomers in HeLa cells.

Mechanism of Uptake

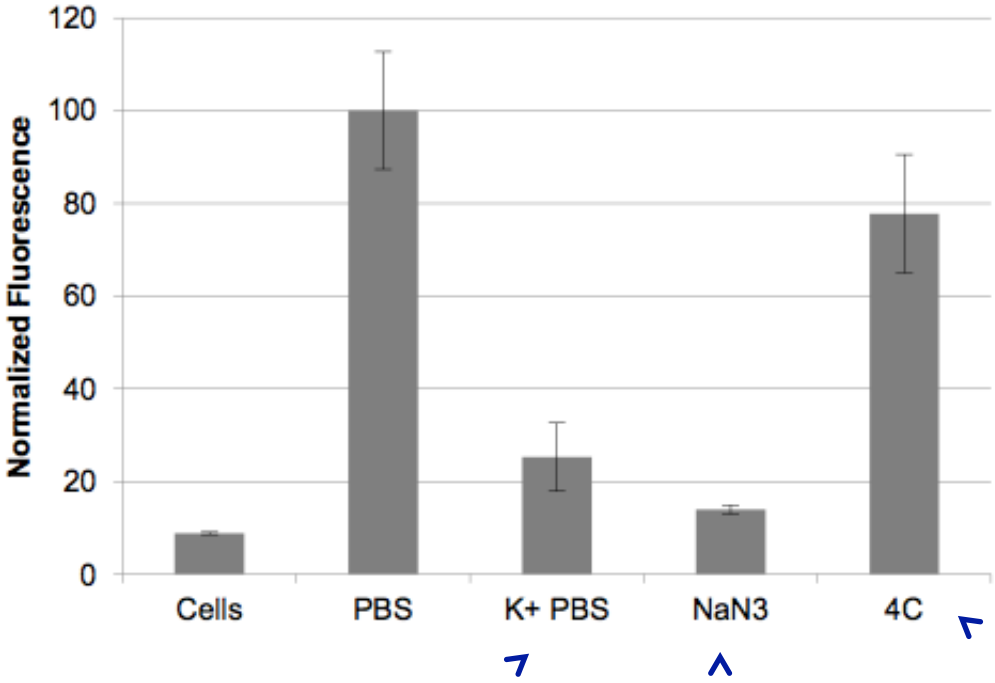

Figure S10. Mechanistic study of uptake of Dansyl-HexPhos8 oligomer **6a** in HeLa cells. Cells were pre-treated with designed conditions and the uptake measured by flow cytometry.

A condition known to reduce the membrane potential
: 75% reduction in uptake

A condition which attenuates endocytotic entry
: 25% reduction in uptake

Inhibits ATP-dependent processes witch inhibits both endocytosis and neutralizes the membrane potential by disabling Na-K exchange pumps
: significant (86%) reduction in uptake

Delivery of Thiol-Reactive Probes

Clickable conjugation strategy

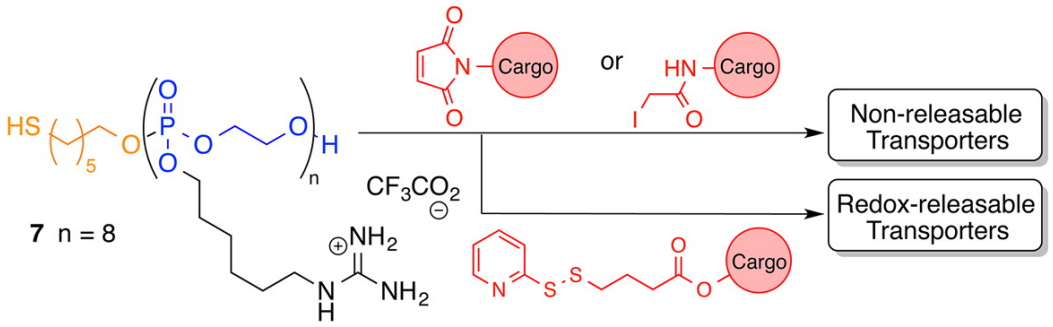

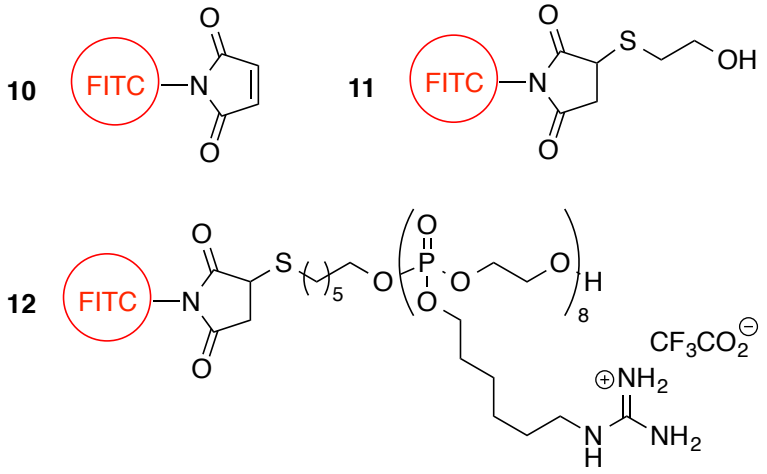

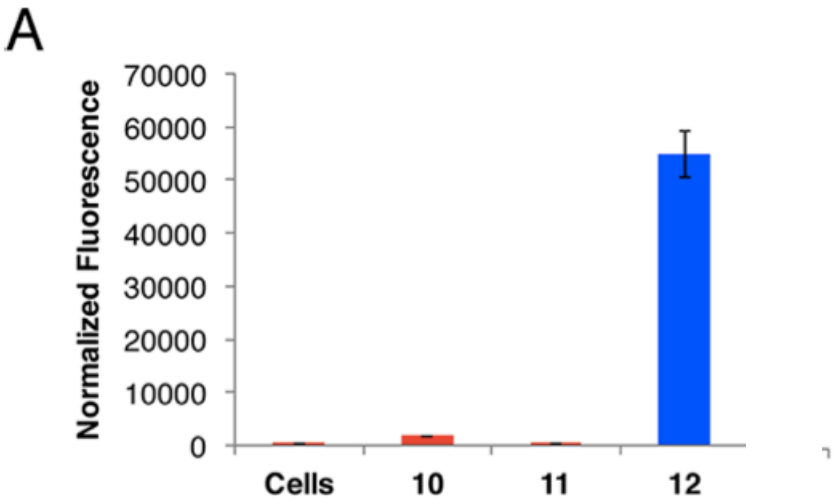

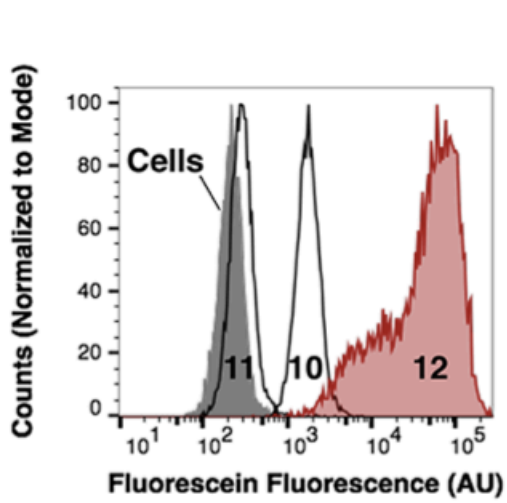

Uptake of FL-maleimide to HeLa cells by click-coupling to thiol-initiated HexPhos oligomer 8 determined by flow cytometry.

Representative flow cytometry histogram showing a complete shift in population fluorescence for cells treated with FL-HexPhos conjugate **12**.

Intracellular Localization of HexPhos Oligomer 12

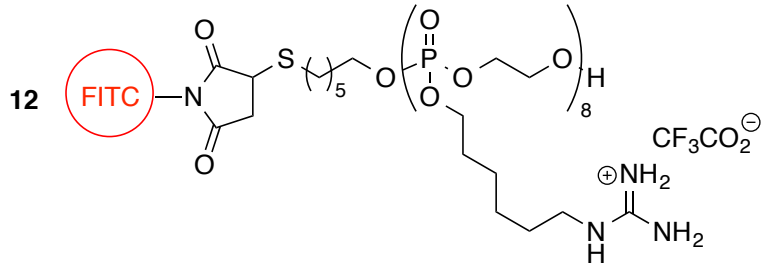

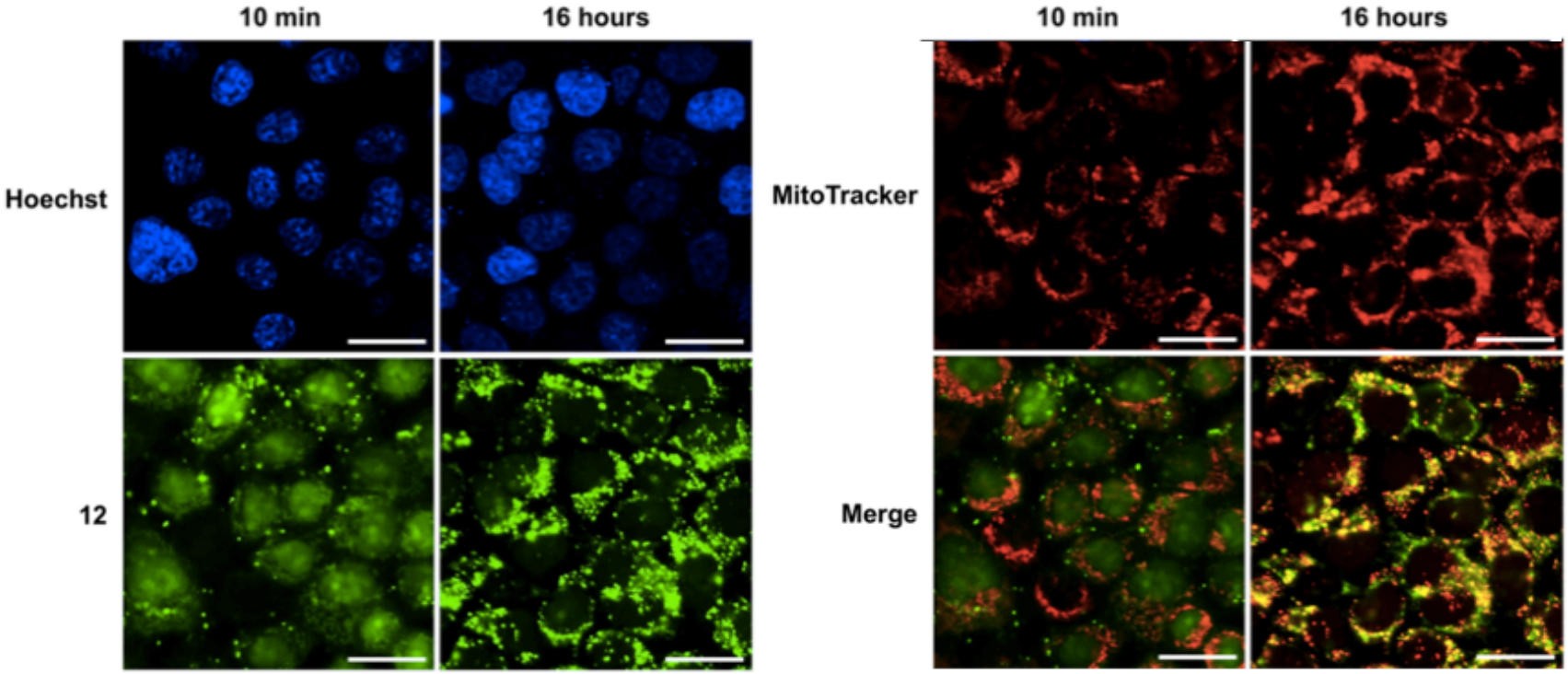

Confocal microscopy images of HeLa cells treated with FL-HexPhos8 conjugate **12** (10 µM) for 10 min. Cell nuclei were counterstained with Hoechst 33342 and mitochondria stained with MitoTracker prior to imaging. Images were taken 10 min and 16 h following treatment. Scale bars represent 25 µm.

Synthesis and Evaluation of Paclitaxel (PTX)-HexPhos Conjugate

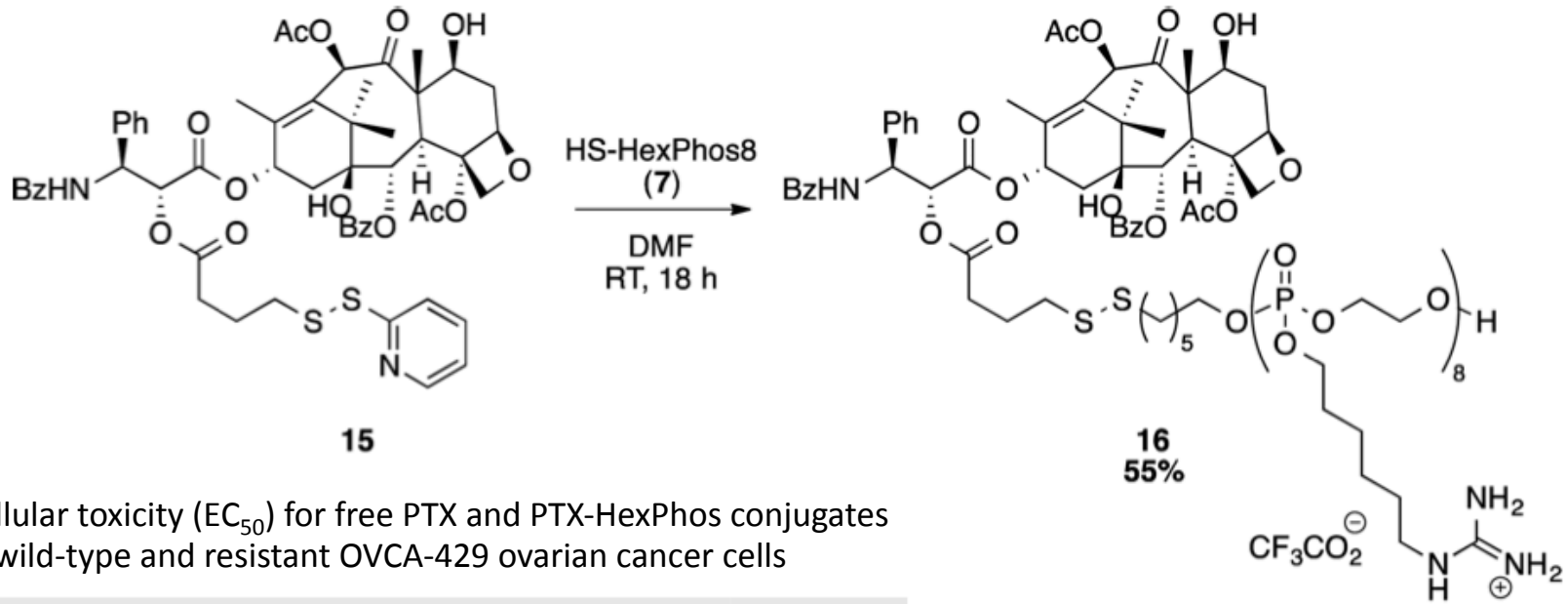

15

16
55%

Cellular toxicity (EC_{50}) for free PTX and PTX-HexPhos conjugates in wild-type and resistant OVCA-429 ovarian cancer cells

compound	EC_{50} (μM)[a]		resistance factor[b]
	OVCA-429 (wild-type)	OVCA-429T (resistant)	
PTX Alone (**14**)	0.051 ± 0.037	>20	>400
PTX-HexPhos8 (**16**)	0.26 ± 0.073	1.4 ± 0.45	5.2
HS-HexPhos8 (**7**)	–	13 ± 2.9	–

[a]Determined by treating cells for 20 min with compounds, followed by a wash and incubation in drug-free media for 72 h and determining viability by MTT assay. All values are the result of three separate experiments, each performed in triplicate with error being the standard deviation. [b]Resistance factor = EC_{50} (wild-type)/EC_{50} (resistant)

16

Summary

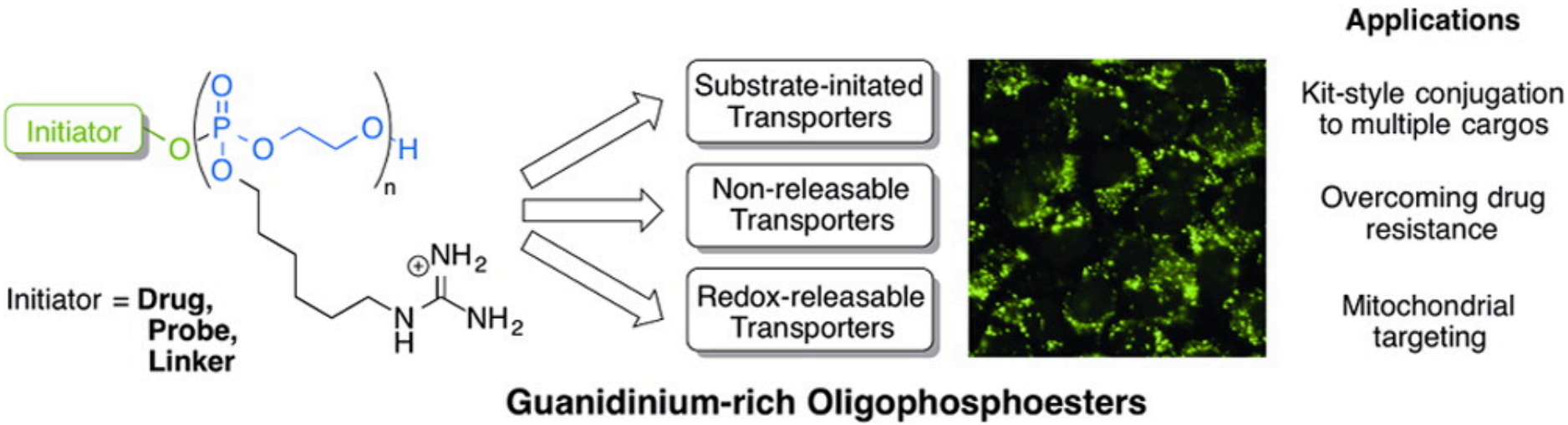

- The design, synthesis, and biological evaluation of a new class of guanidinium-rich oligophosphoester delivery vehicles in multiple delivery applications have been described
- Cellular uptake is substantially higher than the previously reported oligoarginine and oligocarbonate systems
- Preparation of HexPhos monomer and oligomerization process – in Glovebox
- Possibilities for dermatological applications?

J. Am. Chem. Soc. Ahead of Print DOI: 10.1021/jacs.5b13452